Numerical Study of Water Effects on the Laminar Burning Velocity of Methanol

Kun Liang

Department of Engineering and Design, University of Sussex, Brighton BN1 9QT, UK

Tel: +44 1273 678573. Email address: kun.liang@sussex.ac.uk

Abstract

Using light alcohols in spark-ignition engines can improve energy security, engine performance and pollutant emissions. Methanol has gained popularity due to its ease in production compared to ethanol. Methanol could absorb water easily. In the present work, the adiabatic laminar burning velocity of methanol containing water is investigated both experimentally and numerically. Numerical simulations using CHEMKIN-PRO were undertaken to predict the burning velocities of six mixtures with different water volume fractions (up to 0.6) from the latest San Diego chemical-kinetic mechanism. The burning velocities of three mixtures with different water volume fractions (up to 0.4) were measured using a constant volume vessel and a Schlieren imaging system for a wide range of temperature (380-450 K), pressure (100-400 kPa) and equivalence ratio (0.7-1.4). Results showed a decrease in burning velocity with pressure and an increase with temperature. Water as a diluent led to reduction of the burning velocity. The chemical-kinetic mechanism over predicts the burning velocity.

Keywords: Methanol, Laminar burning velocity, Water, Constant volume, Chemical kinetic mechanism, Schlieren imaging

1. Introduction

Using light alcohols in spark-ignition engines can improve energy security, engine performance and pollutant emissions. Sustainable liquid alcohols, such as ethanol and methanol, are largely compatible with the existing fuelling and distribution infrastructure and are easily stored in a vehicle **[1]**. Methanol can be produced from a wide range of renewable sources such as gasification of wood, agricultural by-products and urban waste, in addition to fossil fuels based feedstock (coal and natural gas). For the purposes of energy sustainability and low carbon, methanol has been widely used in spark ignition engines in some countries like China and Iceland, as a single component and blend with gasoline **[2]**. Due to the high octane rating, high latent heat and low combustion temperatures, the power and efficiency is significantly higher for methanol (and ethanol) compared to gasoline. This is certainly true for highly pressure-charged engines, where aggressive downsizing is possible on these alcohols **[3]**.

Methanol is very hygroscopic and even purified methanol by distillation will absorb water vapour directly from the atmosphere. Water in methanol will further improve the anti-knock rating. However, it dilutes the calorific value of methanol, and may cause phase separation of methanol-gasoline blends. The water is expected to reduce the burning velocity, the flame

stability and the flammability range, all of which would be adverse to the performance of the engine.

The laminar burning velocity is a fundamental property of fuel for spark ignition engines, which can also be used to validate the chemical-kinetic mechanism and estimate the turbulent burning velocity. The laminar burning velocity depends on the initial pressure, mixture temperature and equivalence ratio of the unburned mixture.

Many researchers have conducted experimental studies of pure methanol using different methods: (1) constant volume vessel approach has been used by Saeed and Stone **[4]**, Metghalchi and Keck **[5]**, Gulder **[6]**, Liao et al. **[7, 8]**, Zhang et al. **[9, 10]**, and Beeckmann et al. **[11**. Note that **[4, 7, 8, 9, 10 and 11]** used optical access to the combustion vessel; (2) counter flow flame configuration was used by Davies and Law **[12]** and Egolfopoulos et al. **[13]**; (3) Bunsen burner was used by Gibbs and Calcote **[14]**; (4) heat flux burner was adopted by Sileghem et al. **[15]** and Vancoillie et al. **[16]**; (5) meso-scale diverging channel was recently used by Katoch et al. **[17]**. Constant volume vessel was also used by **[18 and 19]**.

Numerical studies of laminar burning velocity has also been widely conducted but not for methanol/water mixtures up to date. CHEMKIN based simulations can be used to predict laminar burning velocity from different reaction mechanisms. The most widely used mechanisms for development of alcohol chemistry are Li et al. **[20]** and San Diego mechanism **[21]**. Li et al. **[20]** presented an updated C1 mechanism for methanol (CH3OH) combustion, which appeared to over predict the burning velocity as shown by Katoch et al. **[17]**. The San Diego mechanism **[21]** is being frequently updated by latest published experimental data. The correlations of burning velocity from experiments using constant volume vessel for methanol/water mixtures have been reported by Liang and Stone **[22]**. Though Katoch et al. **[17]** states that the San Diego mechanism tends to over predict the burning velocity for rich mixture of methanol and air, it is still unknown that how burning velocity varies for methanol when water (H2O) is added as a diluent. Therefore, the capability of this mechanism in modelling methanol/water combustion still needs further validation. This paper presents numerical work on laminar burning velocity using CHEMKIN-PRO **[23]** in comparison with results from Schlieren imaging analysis that has not been reported in **[22]**.

2. Computational Simulation

The numerical simulations of laminar premised flames were conducted using steady-state, one-dimensional freely propagating laminar flame model in CHEMKIN-PRO. As the adiabatic flame speed was determined from the heat flux method, no radiative heat loss was considered in simulations. The hybrid time-integration/Newton-iteration technique with adaptive meshes and mixture-averaged transport parameters is applied to solve the steady-state mass, species and energy conservation equations of the flames.

A one-dimensional flow with uniform inlet conditions were assumed. The governing conservation equations for the freely propagating flame are as follow:

For continuity: $$\dot{M} = \rho u A \quad (1)$$

where $\dot{M}$ is the mass flow rate, ρ is the mass density, u is the velocity of the fluid mixture and A is the cross-sectional area of the stream tube encompassing the flame normalised by the burner area.

For energy: $$\dot{M}\frac{dT}{dx} - \frac{1}{c_p}\frac{d}{dx}\left(\lambda A \frac{dT}{dx}\right) + \frac{A}{c_p}\sum_{k=1}^{K}\dot{\omega}_k h_k W_k \quad (2)$$

where x is the spatial coordinate, T is the temperature, c_p is the constant-pressure heat capacity of the mixture, λ is the thermal conductivity of the mixture, $\dot{\omega}_k$ is the molar rate of production by chemical reaction of the *k*th species per unit volume, h_k is the specific enthalpy of the *k*th species, and W_k is the molecular weight of the *k*th species.

For species: $$\dot{M}\frac{dY_k}{dx} + \frac{d}{dx}(\rho A Y_k V_k) - \mathrm{A}\dot{\omega}_k W_k = 0 \quad (3)$$

where Y_k is the mass fraction of the *k*th species and V_k is the diffusion velocity of the *k*th species.

For equation of state: $$\rho = \frac{P\bar{W}}{RT} \quad (4)$$

where $\bar{W}$ is the mean molecular weight of the mixture and *R* is the universal gas constant.

The computation domain was set from -2 cm to 10 cm to ensure the boundaries sufficiently far from the flame itself so that there was negligible diffusion of heat and mass through the boundary. The relative gradient and curvation parameters for the grid refinement are set to be 0.1 to ensure that the number of grids were over 150 for each condition. This number proved sufficient in rendering the simulation as grid-independent. The fixed-flame coordinate system is established by explicitly constraining the gas temperature to stay at the initial fixed value at one grid point in the computational domain.

For the pre-mixed laminar flame speed model in CHEMKIN-PRO, chemistry set components required include thermochemical data, gas-phase chemistry (chemical reactions and rate parameters) and transport data. For the present work, the latest San Diego mechanism pulished on 2016-12-14 **[21]** was employed, which has 57 species and 247 elementary reactions. The chemistry set of the mechanism was created in 'Pre-Processing'. A total number of 504 computational simulations were conducted in CHEMKIN-PRO. Table 1 listed the test conditions for methanol/water mixture. In 'C1-Inlet' of the model, equivalence ratio and fractions of each species can be defined along with mass flow rate. The burning velocity by using CHEMKIN-PRO is thus named as 'CHEMKIN-PRO' for comparison with 'Schlieren' results. The equivalence ratio is the ratio of the fuel-to-air ratio to the stoichiometric fuel-to-air ratio. Equivalence ratio over 1 means rich mixture.

Table 1 Simulation conditions of burning velocity for methanol/water mixtures

Water volume fraction	Initial pressure (kPa)	Initial temperature (K)	Equivalence ratio
0, 0.1, 0.2, 0.3, 0.4, 0.5, 0.6	100, 200, 400	300, 380, 450	0.7, 0.8, 0.9, 1.0, 1.1, 1.2, 1.3, 1.4

3. Optical Measurement

3.1 Constant Volume Vessel and Schlieren Imaging System

The constant volume vessel method is capable of exploiting the increase in pressure and the resulting increase in unburned gas temperature. Values of the burning velocity can be calculated for multiple temperatures and pressures from a single experiment as the pressure rise causes an isentropic temperature increase in the unburned gas. Therefore, the burning velocity can be determined from the pressure trace inside the combustion bomb (shown in Fig. 1a) by assuming a smooth spherical flame front and an appropriate combustion mode. The details of the bomb have been reported by Liang and Stone **[22]**.

A Schlieren imaging system was adopted for the purpose of imaging the flame front to determine flame speed in the initial stages of combustion and also for detection of cellularity in the later stages of combustion when the pressure rise is more significant. The Schlieren system for this work is a folded z-type arrangement shown in Fig. 1b. The system uses two oppositely tilted off-axis spherical mirrors to produce the collimated beam. Increasing pressure results in a change in density across the flame front and the flame front thickness, both of which affect the density gradient and hence the darkness of the detected Schlieren edge. The illumination source used is a 1 W green Prolight Power Star/O LED. The pressure vessel had a pair of windows with 40 mm diameter along the optical axis (see Fig. 1a) to allow the Schlieren imaging system. The Schlieren images were recorded using a Photron 1024 PCI high speed camera with a 512*512 pixel resolution, allowing a frame rate of 3000 frame per second (fps). The measured flame speed can be then used to determine the laminar burning velocity for validating the numerical simulation described in Section 2.

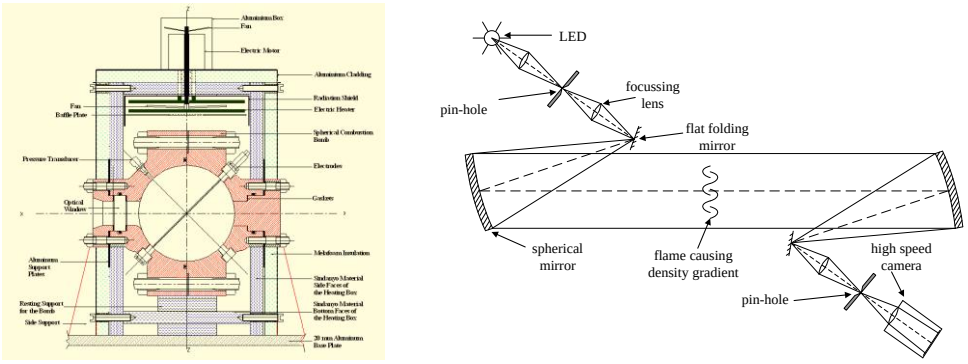

(a) (b)

Fig. 1 Schematic of the constant volume combustion bomb with optical window for Schlieren imaging system (a) **[22]** and arrangement of folded z-type Schlieren imaging system (b)

A total of 144 experiments were conducted over a wide range of initial temperatures (380 K and 450 K), pressures (100 kPa, 200 kPa and 400 kPa) and equivalence ratios (0.7 – 1.4) for 3 methanol/water blends (W0, W20, and W40). W0 is pure methanol. W20 and W40 mean water volume fractions of 0.2 and 0.4, respectively.

The propagation speed of a spherical flame can be derived from the flame radius versus time as below:

$$S_f = \frac{dr}{dt} \tag{5}$$

where r is the radius of the flame recorded by Schlieren imaging.

The flame stretch rate can be calculated as

$$\alpha = \frac{1}{A}\frac{\mathrm{d}A}{\mathrm{d}t} = \frac{2dr}{rdt} \tag{6}$$

where A is the area of the flame surface.

Removing the stretched flame speed data affected by ignition energy and electrodes during the early stage of flame development gives a linear correlation line for the stretched flame speed and the flame stretch rate as shown in the Fig. 2. The unstretched flame speed S_s is found by extrapolating back to the case of zero stretch (α =0). It can be seen that the effect of the stretch rate on the burning velocity is not significant.

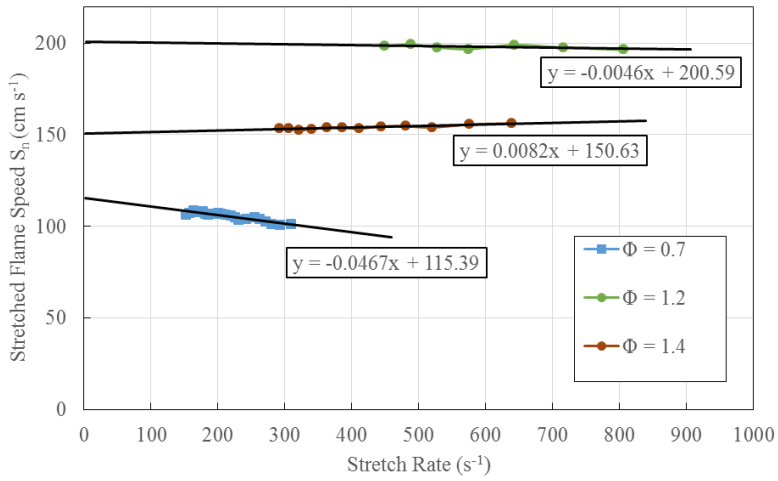

Fig. 2 Extrapolations of unstretched flame speed (S_s) for W0 at T_u = 380 K and P_u = 200 kPa

The unstretched laminar burning velocity u_l can then be calculated according to

$$u_l = \rho_b S_s / \rho_u \tag{7}$$

where ρ_b and ρ_u are densities for burned gas and unburned gas respectively. The laminar burning velocity calculated from Schlieren imaging data is named as 'Schlieren'.

The Schlieren imaging data were also used for detecting the cellularity so that the data set for correlation can exclude the cellular data as has been described by Liang and Stone **[22]**. Cellularity describes the phenomenon whereby a flame front develops an instability causing deviation from a smooth flame front to 'cellular' structure. These represent regions of intensified or weakened burning, caused by local inhomogeneity in the mixture composition within the flame front, meaning that the burning rate is no longer uniform over the flame front resulting in the uneven surface. Fig. 3 shows Schlieren images of the flame front of W0 at 20 ms for different initial pressures (P_u) and equivalence ratios (Φ) when the initial temperature is 450 K. At the initial pressure of 100 kPa, a smooth flame front is observed at three equivalence ratios. When the initial pressure increases to 200 kPa, the cellular structure at the flame front begins to occur for stoichiometric and the rich mixtures. As the initial pressure increases to 400 kPa, a strong cellular flame front appears even for lean mixture. For a specific equivalence ratio, the cellular flame structure develops more easily with increased initial pressure.

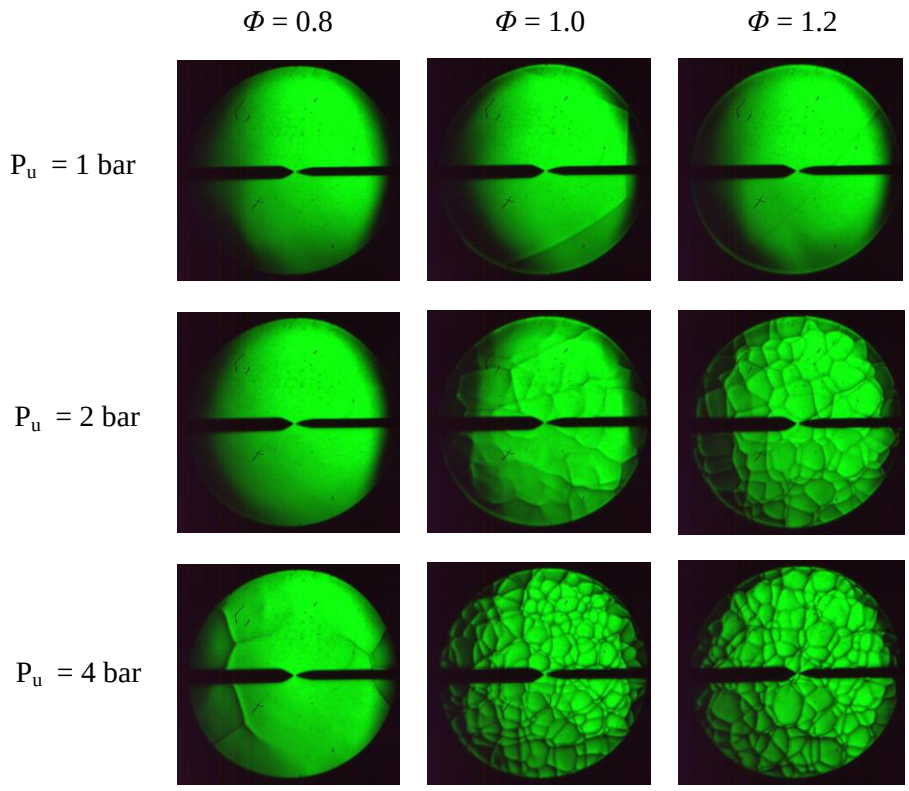

Fig. 3 Schlieren images of the flame front of W0 at 20 ms for different initial pressures (P_u) and equivalence ratios (Φ) at T_u = 450 K.

4. Results and Discussions

4.1 Effect of Water

The laminar burning velocity of stoichiometric methanol and air mixture with different water fraction from 0 to 0.6 is shown in Fig. 4 using three methods described above for initial temperature of 450 K and initial pressure of 200 kPa. Water as a diluent clearly reduce the burning velocity of methanol linearly. Schlieren results show that the burning velocity

decreases from 80 cm s^{-1} to 46 cm s^{-1} when water fraction increase from 0 to 0.4. The CHEMKIN results using San Diego mechanism over predict the burning velocity by 5%.

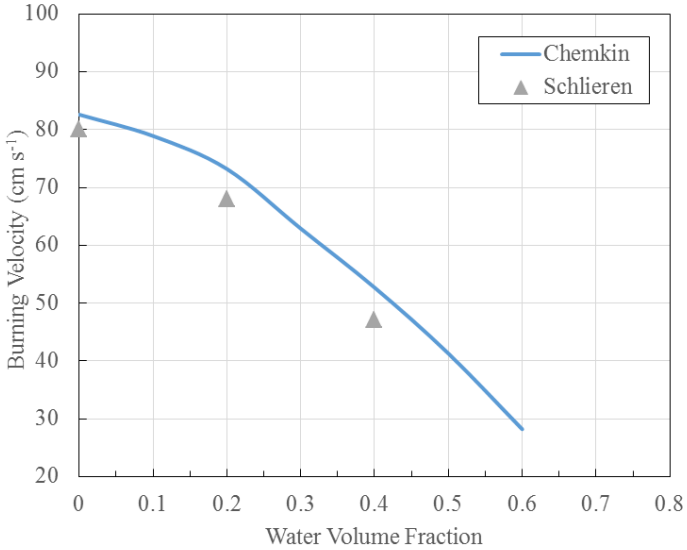

Fig. 4 Laminar burning velocity variation of stoichiometric methanol/water and air mixtures against water fraction in volume using correlation, Schlieren and CHEMKIN methods at T_u = 450 K and P_u = 200 kPa

Fig. 5 shows CHEMKIN results for three methanol/water mixtures at different equivalence ratios. Increasing water fraction shifts the peak buring velocity towards stoichiometric probably due to the cooling effect of the increased water volume fraction lowering the adiabatic flame temperature leading to less dissociation and hence, a peak burning velocity occurring closer to stoichiometric.

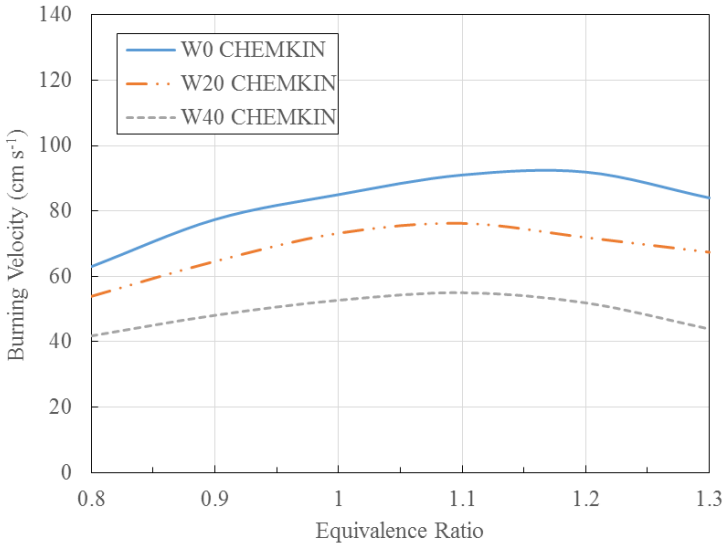

Fig. 5 CHEMKIN results for the laminar burning velocity of methanol with different water fractions at T_u = 450 K and P_u = 200 kPa

4.2 Effect of Temperature

Fig. 6 shows the CHEMKIN simulation for the laminar burning velocities at elevated temperatures for stoichiometric methanol/water/air mixtures at P_u = 200 kPa. Increasing the temperature of the mixture results in a faster burning velocity as expected. It can be seen that temperature has hardly effect on the difference between methanol and hydrous methanol. This may not be realistic because high temperature leads to increased dissociation, which would affect the burning velocity.

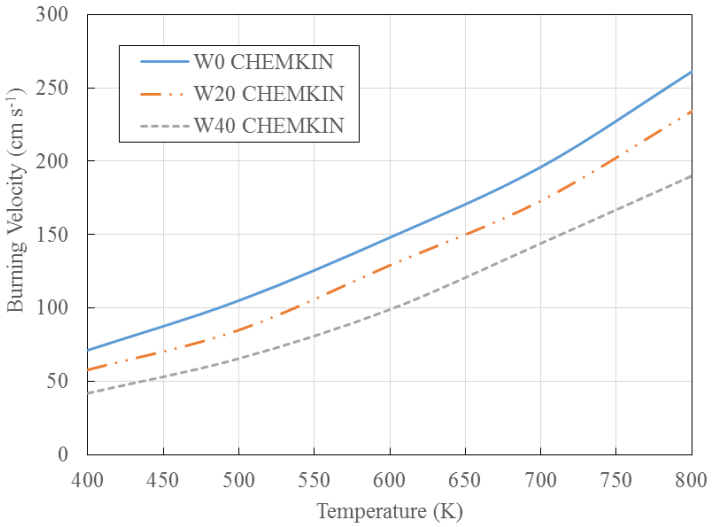

Fig. 6 CHEMKIN results for the laminar burning velocity against temperature evaluated at 200 kPa for stoichiometric mixtures of methanol with different water fractions

4.3 Effect of Pressure

Fig. 7 shows the effect of pressure on the burning velocity of methanol with different water fractions with initial temperature of 380 K. As expected, increasing the pressure results in a lower laminar burning velocity. The peak burning velocity for W40 is lower than the minimum for W0 as shown from both Schlieren and CHEMKIN simulation. This indicates that adding 40% water (by volume) would make the methanol unsuitable for a spark ignition engine. Schlieren imaging analysis results show that the peak burning velocity shifts towards stoichiometric as pressure increases. This is because increased pressure would lead to less dissociation. However, CHEMKIN simulation predicts an opposite trend. This further indicates that the San Diego mechanism requires improvement.

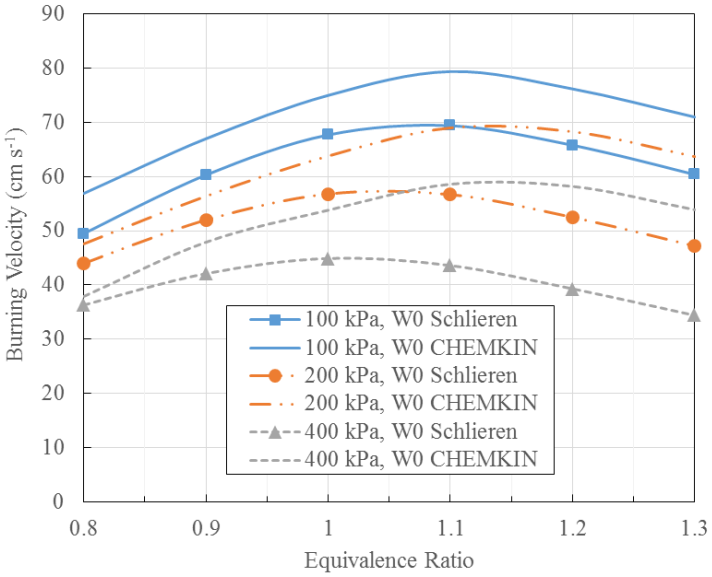

Fig. 7 Comparison between the Schlieren and CHEMKIN results for the laminar burning velocity of methanol with different water fractions at different pressures (P_u) and T_u = 380 K

5. Conclusions

The effect of water on the laminar burning velocity of methanol has been investigated by using a constant volume combustion bomb associated with a Schlieren imaging system and computational simulation using CHEMKIN-PRO based on the latest San Diego chemical kinetic mechanism. The data reported here has the expected trends:

(1) Increasing water fraction reduces the burning velocity of methanol. Methanol with water volume fraction of 0.4 (W40) appears to burn significantly more slowly. Correlation results in **[22]** show that adding more water will shift the equivalence ratio of the peak burning velocity away from stoichiometric due to more dissociation. However, CHEMKINN model using San Diego mechanism shows an opposite trend as shown in Fig. 5. San Diego mechanism over predict the burning velocity by 5% for stoichiometric mixture. This is within an acceptable range.

(2) Schlieren imaging data shows that the flame front of W0 becomes cellular very quickly after the ignition of a rich mixture. High initial pressure and rich mixture will lead to an early cellular flame for a constant initial temperature.

(3) Both Schlieren and CHEMKIN model show that higher pressures lead to a lower laminar burning velocity. Increasing the temperature increases the burning velocity. Schlieren result shows that the peak burning velocity appears to be close to equivalence ratio of 1.1 for pure methanol (W0), which agrees with most of the available results in the literature. However, CHEMKIN model shows a higher equivalence ratio at peak burning velocity.

(4) Though the San Diego mechanism can predict the burning velocity, it is strongly suggested that the mechanism should be updated, particularly for high temperature as well as the effect of pressure on the position of peak burning velocity.

Acknowledgement

The author is very grateful to Prof Richard Stone at the University of Oxford for support on the measurements and discussions on the experimental results.

References

[1] Vancoillie J, Demuynck J, Sileghem L, Van De Ginste M, Verhelst S, Brabant L, and Van Hoorebeke L. The potential of methanol as a fuel for flex-fuel and dedicated spark-ignition engines. Applied Energy 2013; 102: 140–149.

[2] Wang X, Ge Y, Zhang C, Tan J, Hao L, Liu J, and Gong H. Effects of engine misfire on regulated, unregulated emissions from a methanol-fueled vehicle and its ozone forming potential. Applied Energy 2016; 177: 187–195.

[3] Liu SH, Eddy C, Hu, TG, and Wei YJ. Study of spark ignition engine fueled with methanol/gasoline fuel blends. Applied Thermal Engineering 2007; 27: 1904-1910.

[4] Saeed K, and Stone CR. Measurements of the laminar burning velocity for mixtures of methanol and air from a constant-volume vessel using a multizone model. Combust Flame 2004;139:152–66.

[5] Metghalchi M, and Keck JC. Burning velocities of mixtures of air with methanol, isooctane, and indolene at high pressure and temperature. Combust Flame 1982; 48: 191–210.

[6] Gulder ÖL. Laminar burning velocities of methanol, isooctane and isooctane/methanol blends. Combust Sci Technol 2007; 33: 179–92.

[7] Liao SY, Jiang DM, Huang ZH, Shen WD, Yuan C, and Cheng Q. Laminar burning velocities for mixtures of methanol and air at elevated temperatures. Energy Convers Manage 2007; 48: 857–63.

[8] Liao SY, Jiang DM, Huang ZH, and Zeng K. Characterization of laminar premixed methanol–air flames. Fuel 2006; 85: 1346–53.

[9] Zhang Z, Huang Z, Wang X, Xiang J, Wang X, and Miao H. Measurements of laminar burning velocities and Markstein lengths for methanol–air–nitrogen mixtures at elevated pressures and temperatures. Combust Flame 2008; 155: 358–68.

[10] Zhang Z, Huang Z, Wang X, Zheng J, Miao H, and Wang X. Combustion characteristics of methanol–air and methanol–air–diluent premixed mixtures at elevated temperatures and pressures. Appl Therm Eng 2009; 29: 2680–8.

[11] Beeckmann J, Cai L, Pitsch H, Experimental investigation of the laminar burning velocities of methanol, ethanol, n-propanol, and n-butanol at high pressure. Fuel 2014; 117: 340–350.

[12] Davis S, and Law CK. Determination of and fuel structure effects on laminar flame speeds of C1 to C8 hydrocarbons. Combust Sci Technol 1998; 140: 427–49.

[13] Egolfopoulos FN, Du DX, and Law CK. A comprehensive study of methanol kinetics in freely-propagating and burner-stabilized flames, flow and static reactors, and shock tubes. Combust Sci Technol 1992; 83: 33–75.

[14] Gibbs GJ, Calcote HF. Effect of molecular structure on burning velocity. J Chem Eng Data 1959; 4: 226–37.

[15] Sileghem L, Alekseev VA, Vancoillie J, Nilsson EJK, Verhelst S, Konnov AA. Laminar burning velocities of primary reference fuels and simple alcohols. Fuel 2014; 115: 32–40.

[16] Vancoillie J, Christensen M, Nilsson EJK, Verhelst S, Konnov AA. Temperature dependence of the laminar burning velocity of methanol flames. Energy Fuels 2012; 26: 1557–64.

[17] Katoch A, Asad A, Minaev S, Kumar S. Measurement of laminar burning velocities of methanol–air mixtures at elevated temperatures. Fuel 2016; 182: 57–63.

[18] Liao SY, Jiang DM, Cheng Q, Gao J, Huang ZH, and Hu Y. Correlations for laminar burning velocities of liquefied petroleum gas–air mixtures. Energy Conversion and Management 2005; 46 (20): 3175–3184.

[19] Razus D, Oancea D, Brinzea V, Mitu M, and Movileanue C. Experimental and computed burning velocities of propane–air mixtures. Energy Conversion and Management 2010; 51 (12): 2979–2984.

[20] Li J, Zhao Z, Kazakov A, Chaos M, Dryer FL, and Scire JJ. A comprehensive kinetic mechanism for CO, CH2O, and CH3OH combustion. International Journal of Chemical Kinetics 2007; 39:109–36.

[21] Chemical-Kinetic Mechanisms for Combustion Applications, San Diego Mechanism web page, Mechanical and Aerospace Engineering (Combustion Research), University of California at San Diego (http://combustion.ucsd.edu).

[22] Liang, K., and Stone, C.R., Laminar Burning Velocity Measurement of Hydrous Methanol at Elevated Temperatures and Pressures. Fuel 2017; 204: 206-213.

[23] CHEMKIN-PRO Release 15083 Tutorial Manual. Reaction Design, 2008.